Mode-locked far-infrared p-Ge laser using an offset rf electric field for gain modulation

A. V. Muravjov, R. C. Strijbos, C. J. Fredricksen, H. Weidner, W. Trimble, A. Jamison, S. G. Pavlov,* V. N. Shastin,* and R. E. Peale

Physics/CREOL, University of Central Florida, Orlando, FL 32816, 407-823-3076, FAX: 407-823-5112, rep@physics.ucf.edu

*Institute for Physics of Microstructures, Russian Academy of Sciences, Nizhny Novgorod 603600, Russia.

Abstract

Active mode locking of the far-infrared p-Ge laser is achieved via gain modulation with an rf electric field applied at one end of the crystal parallel to the Voigt-configured magnetic field. A small intrinsic voltage is observed between the rf contacts during lasing which significantly impairs the gain and also the achievable intensity and duration of mode-locked pulses. This voltage is directly compensated by applying a bias to the rf contacts. First results give mode-locked pulse durations of ~ 200 ps.

Key Words

(140.3070) Infrared and far-infrared lasers; (140.5960) Semiconductor lasers; (140.4050) Mode-locked lasers; (300.6270) Spectroscopy, far infrared.

Recent efforts to improve p-Ge far-infrared lasers (50 - 140 cm^{-1}) have concentrated on increasing the duty cycle[1], use of permanent magnets[2] and closed cycle refrigerators[3] to eliminate liquid cryogens, deep donor doping[4,5] to separate impurity absorption from the gain spectrum, and active mode-locking[6]. Motivation has been a lack of a compact solid state laser between millimeter and infrared wavelengths and increasingly important applications for THz radiation. This paper reports active mode locking, new spectroscopic results, and important new observations concerning electrical gain control.

Basic principles are presented briefly. Fig. 1 shows allowed energy surfaces vs momentum k_X,k_Y for light (upper) and heavy holes. The upper plot boundary is the threshold for inelastic optical-phonon emission, which is the dominant scattering process at low temperatures in pure Ge. The surfaces are calculated in a parabolic approximation including band warping. Fig. 2 presents light and heavy hole orbits calculated numerically from their equation of motion when driven by the Lorentz force for the given crossed electric- and magnetic-field vectors. The axes in Figs. 1 and 2 are the same. For certain ratios E/B, light holes can never reach the optical phonon threshold while heavy holes do, and then light holes have a much longer lifetime. After emitting an optical phonon, heavy holes can add to the accumulated carriers on the light hole surface, thus providing a population inversion on direct optical transitions from light to heavy hole subbands. From Fig. 1 a large gain bandwidth ($\Delta\omega/\omega \sim 1$) is expected with promising consequences for tunability and short-pulse generation ($\tau_{min} \sim 1/\Delta\omega \sim$ ps) [7].

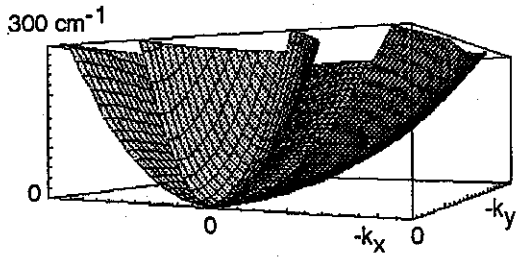

Fig. 1. Light and heavy hole energy surfaces vs kx,ky up to the optical phonon scattering threshold.

OSA TOPS Vol. 18 Radiative Processes and Dephasing in Semiconductors, D. S. Citrin (ed.)

For experiments, single-crystal, Ga-doped, p-Ge with a concentration of 7 x 10^{13} cm^{-3} was cut into rectangular bars with a cross section of 5 x 7 mm^2. Ohmic contacts made by Al-diffusion covering opposite lateral sides of the crystals (5 x L mm^2) are used for applying electric field pulses $\mathbf{E}_{appl}$ from a low duty thyratron pulser. The crystal ends were polished parallel to each other within 1' accuracy and two external copper mirrors were attached to them via 20 μm teflon film (Fig. 3). Crystals were immersed in liquid helium at 4 K.

A crystal with a length L = 28 mm was chosen for spectroscopic studies in Faraday configuration with $\mathbf{E}_{appl} \parallel [1\text{-}10]$, $\mathbf{B}_0 \parallel [110]$, and magnetic field supplied by a superconducting solenoid inside the cryostat. The spectral measurements were made with a Bomem DA8 Fourier spectrometer using the Event-Locked technique[8].

A crystal with length 42.1 mm was chosen for mode locking experiments in Voigt geometry using an external room temperature electromagnet. The field orientations were $\mathbf{E}_{appl} \parallel [1\text{-}10]$ and $\mathbf{B}_0 \parallel [112]$. For local regulation of the orientation and fast modulation of $\mathbf{E}_{appl}$, small additional contacts with a length of ~4 mm were placed perpendicular to the main contacts at one end of the crystal (Fig. 3). Other experimental details are the same as for the first sample.

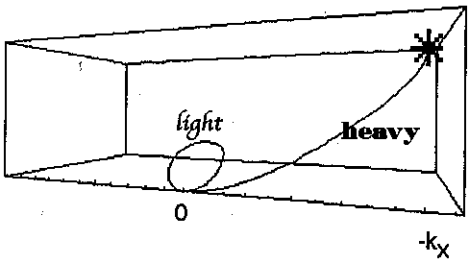

Fig. 2. Calculated light and heavy hole trajectories for E=(-740,0.0)V/cm, B=(0,0,-0.5)T. Axes are the same as in Fig. 1.

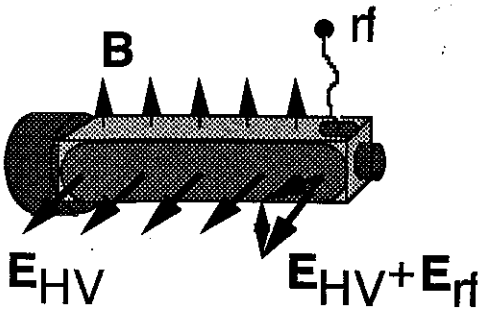

Fig. 3. Diagram of p-Ge laser crystal with rf contacts.

The well known high and low field domains for Ga-doped material have different spectral content. Fig. 4 shows part of the p-Ge laser emission spectrum in the low field region. The high resolution spectrum of the multi-line emission clearly shows the even spacing of the longitudinal mode structure over a wide spectral range, which is an important requirement for mode locking. Although the equidistant spacing, and thus apparent lack of dispersion effects, was already suggested by the narrow linewidth of the homodyne interference product[9], the use of high resolution Event-locked Fourier spectroscopy[8] allows a direct demonstration over a wide spectral range for the first time.

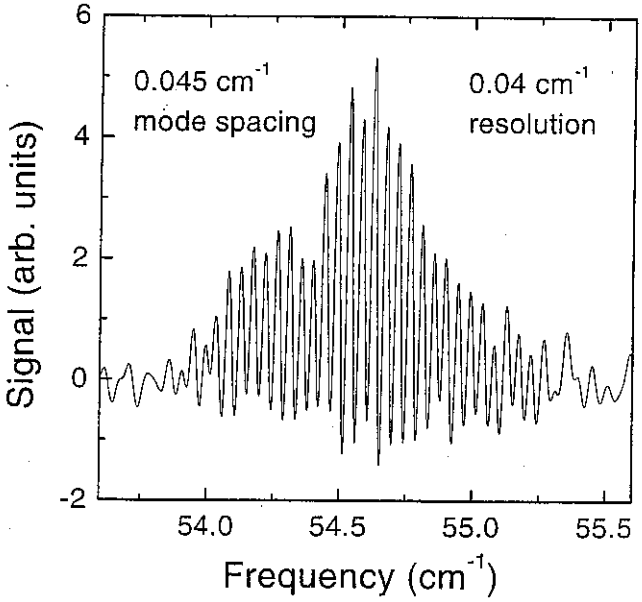

Fig. 4. Fourier spectroscopy of emission from a 28 mm long p-Ge laser showing longitudinal mode structure.

Fig. 5 presents the primary mechanism of active mode locking proposed in [7]. A constant energy surface for light holes (the optical phonon threshold) in (k_x,k_y,k_z)-space is split to show a light-hole orbit calculated as in Fig. 2 but now with the electric field tipped 6° toward the magnetic field. Light holes reach the scattering threshold after a few cycles, thereby reducing the population inversion. We observe experimentally that lasing is extinguished when the applied electric field is tipped ± 3° for our 42.1 mm crystal. By high frequency periodic field tipping at one end of the crystal at half the round trip frequency for photons in the cavity, active mode locking has been achieved (Fig. 3)[6]. Note that gain reduction occurs at twice the applied frequency. Our scheme, presented here, differs from [6] in having a controllable offset voltage in addition to the periodic field perturbation in the direction of the magnetic field. As will be discussed

below, this offset centers the perturbation at the peak of the gain vs.tipping-angle curve, which provides equal temporal spacing for the repeating gain maxima. This last condition is necessary to obtain the shortest possible pulses with the highest possible intensity.

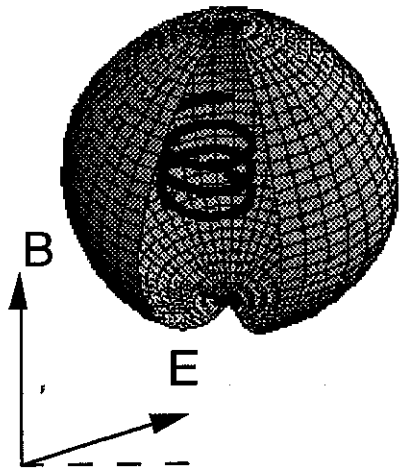

Fig. 5. Constant energy surface (optical phonon scattering threshold) for light holes in k-space. A calculated light hole trajectory for non-orthogonal fields is shown.

It has been shown that even without active mode locking, the circulation of the electromagnetic field in the cavity yields significant periodic output-intensity oscillations, which result from interference of laser modes with random initial phases[10]. The interference pattern differs for each laser shot. This can be observed in the time domain using a whisker-contacted Schottky-diode detector with fast bias-T, amplifier, and transient digitizer. Fig. 6 shows the build up of the laser signal on the Schottky diode. The inset shows the signal for about two round-trip times for a shot with particularly large intensity variations. From these data, a round trip frequency of 905 MHz is determined, which is within 0.3 % of the value calculated from $f=c/(2n_{Ge}L)$, with $n_{Ge} = 3.925$ and $L= 42.1$ mm.

Applying rf power to additional contacts at one end of the sample ($E_{rf} \parallel B$) provides the sinusoidal tipping of the total electric field vector, which should modulate the gain twice per rf cycle. For the crystal used in Fig. 6, the useful rf modulation frequency near 452 MHz permits cheap ham-radio electronics. Since the impedance of the crystal between the rf contacts is expected to be low, high rf power is required. The rf should just overlap the HV pulses to prevent heating. Our UHF system generates clean sub-μs pulses of a 450 MHz signal using a fast switch, and 2-3 μs pulses can be amplified to 800 W with a solid-state amp followed by a tube amp. A resonant tank circuit provides impedance match.

Fig. 7 shows results of applying rf during the laser pulse. The forward rf power required to extinguish lasing is plotted vs. rf frequency in the right insert. At 452.2 MHz, the laser still operates even when the full available forward rf power is applied, indicating that mode-locking should be occurring[11]. Shifting of the modulation frequency by ±0.5 - 1 MHz blocks the lasing completely, because circulating pulses do not remain in phase with the gain modulation. At resonance, the Schottky diode detector signal plotted in Fig. 7 reveals the mode-locked pulse train. The left inset shows 150 ps pulses from a different shot on a time scale similar to the inset of Fig. 6. The basic pattern of pronounced, separated pulses is now repeatable from shot to shot.

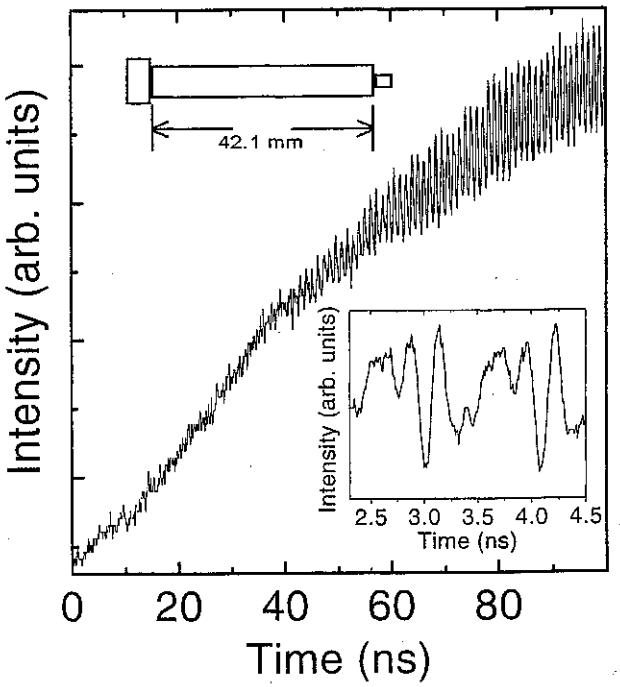

Fig. 6 Transient digitizer trace of p-Ge laser emission onset without rf. The upper inset shows the laser cavity. The lower inset shows the periodic mode structure with 905 MHz round trip frequency.

An important new feature is that for the experiment of Fig. 7, a 20 V bias was applied to the rf contacts in addition to the rf power. This small additional voltage applied between rf contacts has a significant influence on the lasing and mode locking. Changing this bias by ± 5-10 V removes the resonance observed in Fig. 8, indicating that for this particular sample geometry and magnetic field orientation, mode locking is not possible without the bias. The bias is realized according to the

scheme shown in the inset of Fig. 8. The variable resistors change the potentials U1 and U2 of the rf contacts. Fig. 8 presents the U2,U1 parameter space with points enclosing the region of observed lasing. Experiments up to now have been performed without bias (open circle in Fig. 8) and are thus apparently on the border of the lasing region. The system is brought into the center of the region by setting U1-U2 ~ 20 V. Although the absolute value of U2-U1 may depend on sample geometry and field orientations and hence be physically uninteresting, the necessary change Δ(U2-U1) to improve gain characteristics remains important. The significance of this for mode-locking is that rf modulation of U1-U2 should be applied at the peak of the gain-vs-(U2-U1) curve if gain modulation at twice the rf frequency is desired. Note that the intrinsic offset of the modulating electric field (caused by parallel Hall effect[12,13], doping inhomogeneity, or electric-field disturbances caused by the rf contacts) could lead to gain modulation at the applied rf frequency (rather than its second harmonic) at low rf power. Also, even at rf powers sufficient to achieve mode locking anyway, this offset could also cause a broadening of the micropulse duration and a decrease in its intensity.

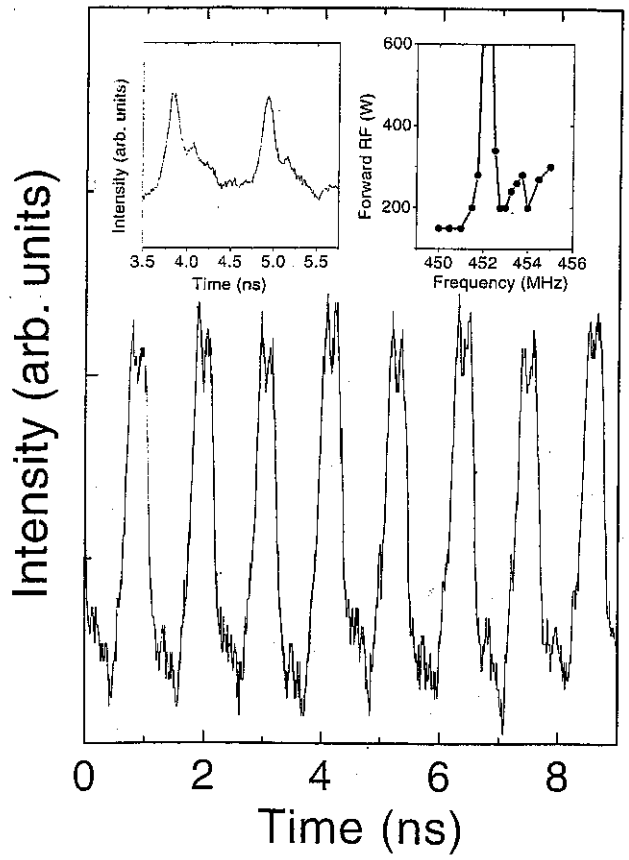

Fig. 7. Output of a mode-locked p-Ge laser. The left inset shows a different shot with 150 ps pulses. The right inset shows the rf resonance at half the round trip frequency.

To clarify the discussion, the mechanism by which the observed bias effect can arise from the Parallel Hall Effect[12,13] is outlined. For B||[112], current components j_L along the magnetic field in perfectly crossed fields are allowed by symmetry, and Monte Carlo simulations indicate that they can be quite substantial for both streaming and accumulated heavy holes in germanium. This leads to charging of the sample sides with the rf electrodes and a Hall-like field E_L along B, which accelerates the light holes and decreases gain. It is possible to compensate this E_L field by tilting B slightly and thus introducing a small component of the applied high voltage along B [12,13]. However, since j_L and thus E_L depend strongly on both the ratio E/B and the relative orientation of **E** and **B**, and the latter are both are inhomogeneous due to the normal Hall Effect, only partial compensation can be achieved in this way. Additional local compensation and gain increase occurs when a bias is applied to the additional contacts.

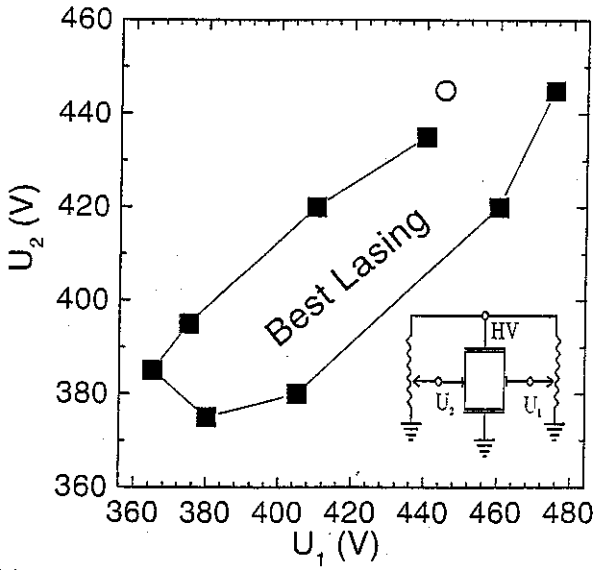

Fig. 8. Scheme of electric-field regulation at rf contacts (inset) together with lasing domain in U1,U2 space.

To gain further insight into the charging effects, U2-U1 was monitored as a function of magnetic field angle $\theta = 90° - \alpha$ with respect to the applied HV field. Fig. 9 plots the change Δ(U2-U1) vs $\Delta\alpha = \alpha - \alpha_0$, where α_0 is the center of the angle range of lasing. Solid symbols indicate how U2,U1 change without the additional resistors, while open triangles give the U2,U1 values for which lasing is optimal for that specific angle. Analysis of the slope in Fig. 9 shows that when the magnetic field is tipped, the electric field in the crystal tries to follow it to maintain the perpendicular condition.

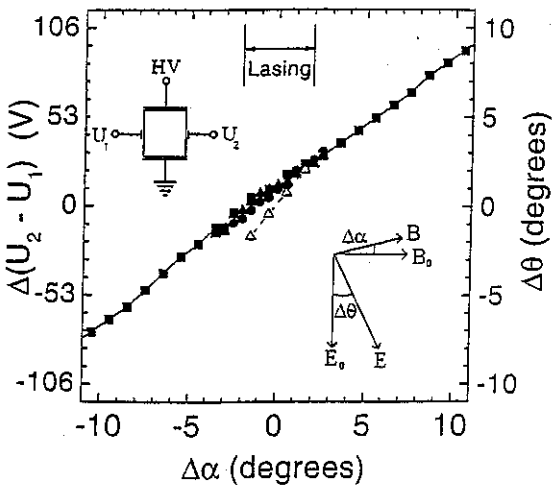

Fig. 9. Effect of magnetic-field tipping on potential between rf contacts.

The measured tendency of the space charge distribution inside the crystal to maintain perpendicularity of fields observed in Fig. 9 can be well understood using a two conductivity model [13], resolving the complicated hole motion into a longitudinal motion along B (determined by mobility $\mu_L=v_L/E_L$) and transverse motion in the plane perpendicular to B (determined by $\mu_T = v_T/E_T$), where v_L, v_T and E_L,E_T are the longitudinal and transverse hole velocities and total electric field components, respectively. It is then easily seen that when μ_L is larger than μ_T, and the magnetic field is tipped, charging of the sample sides with the rf contacts has to occur to maintain parallel current flow along these sides. The potential difference due to this charging is then estimated to be

$$(U1\text{-}U2)/h \approx (\mu_T/\mu_L\text{-}1)E_0 \sin(\alpha) \quad ,$$

where $E_0 = E_{appl}\,(1 + \tan^2\alpha_H)^{1/2}$ is the total transverse electric field E_T in the region between the rf contacts, α_H~40° is the Hall-angle, and h the distance between rf contacts. Thus the slope of the curves will increase when the ratio μ_T/μ_L increases and be zero when the mobilities are equal. Analysis of the slope yields a value for μ_T/μ_L between 3 and 5. The difference between μ_L and μ_T is understood in terms of the significant magnetoresistance decreasing μ_T, and the relatively large contribution of accumulated light holes to μ_L. Further analysis of these curves for different E and B values will be given elsewhere.

In summary, active mode locking of the p-Ge far-infrared laser has been achieved, which results in the generation of an output train of far-infrared pulses with ~200 ps duration. The first high resolution spectrum of longitudinal mode structure over a broad frequency range demonstrates the even mode spacing required for mode-locking. The presence of an electric field due to charging, which partially restores the orthogonality of the total electric and magnetic fields and hence conditions favorable for p-Ge lasing, was measured directly for the first time and explained in terms of a two mobility model. Improvement of the local gain within the active crystal by external control of this transverse bias occurs with important implications not only for active mode locking but for all regimes of p-Ge laser operation.

Acknowledgments

This work was supported by NSF (ECS-9531933) and AFOSR/BMDO (F49620-97-1-0434). Coauthors from IPM thank the Russian Foundation for Basic Research (N96-02-19275).

References

1. E. Bründermann, A. M. Linhart, H. P. Röser, O. D. Dubon, W. L. Hansen, "Miniaturization of p-Ge lasers: progress toward continuous wave operation", Appl. Phys. Lett. 67, 3543-3545 (1995).
2. K. Park, R. E. Peale, H. Weidner, and J. J. Kim, "Voigt-configured p-Ge laser using regular permanent magnets," IEEE J. Quantum Electron. 32, 1203-1210 (1996).
3. E. Bründermann, H. P. Röser, "First operation of a far-infrared p-Germanium laser in a standard closed-cycle machine at 15 Kelvin," Infrared Phys. Technol. 38, 201-203 (1997).
4. E. Bründermann, A. M. Linhart. L. Reichertz, H. P. Röser, O. D. Dubon, W. L. Hansen, G. Sirmain, and E. E. Haller, "Double acceptor doped Ge: A new medium for inter-valence-band lasers", Appl. Phys. Lett. 68, 3075-3077 (1996).
5. G. Sirmain, L. A. Reichertz, O. D. Dubon, E. E. Haller, W. L. Hansen, E. Bründermann, A. M. Linhart, and H. P. Röser, "Stimulated far-infrared emission from copper-doped germanium crystals," Appl. Phys. Lett. 70, 1659-1661 (1997).
6. J. N. Hovenier. A. V. Muravjov, S. G. Pavlov, V. N. Shastin, R. C. Strijbos, and W. Th. Wenckebach, "Active mode locking of a p-Ge hot hole laser," Appl. Phys. Lett. 71, 443-445 (1997).
7. R. C. Strijbos, J. G. S. Lok, and W. Th. Wenckebach, "A Monte Carlo simulation of mode-locked hot-hole laser operation," J. Phys.

Condens. Matter 6, 7461-7468 (1994).
8. H. Weidner and R. E. Peale, "Event-locked time-resolved Fourier Spectroscopy," Applied Spectroscopy 51, 1106-1112 (1997)
9. E. Bründermann, H. P. Röser, A. V. Muravjov, S. G. Pavlov, and V. N. Shastin, "Mode fine structure of the FIR p-Ge intervalenceband laser measured by heterodyne mixing spectroscopy with an optically pumped ring gas laser," Infrared Phys. Technol. 1, 59-69 (1995).
10. A. V. Bespalov, "Temporal and mode structure of the interband p-germanium laser emission," Appl. Phys. Lett. 66, 2703-2705 (1995).
11. R. C. Strijbos, J. H. Blok, J. N. Hovenier, R. N. Schouten, W. Th. Wenckebach, A. V. Muravjov, S. G. Pavlov, and V. N. Shastin, "Active mode locking of a p-Ge light-heavy hole band laser by electrically modulating its gain: theory and experiment," in Proceedings of the 9th Int. Conf. on Hot Carriers in Semiconductors, edited by K. Hess, J.-P. Leburton, and U. Ravaioli (Plenum, New York, 1996), pp. 631-633.
12. R. C. Strijbos, S. I. Schets, and W. Th. Wenckebach, "Appearance of a large 'Hall' current component parallel to B in p-Ge in strong crossed E and B fields," in Proceedings of the 9th Int. Conf. on Hot Carriers in Semiconductors, edited by K. Hess, J.-P. Leburton, and U. Ravaioli (Plenum, New York, 1996), pp. 469-471.
13. R. C. Strijbos, Hole transport effects in p-Ge lasers, PhD thesis, Delft University of Technology, 1997.